(12) INTERNATIONAL APPLICATION PUBLISHED UNDER THE PATENT COOPERATION TREATY (PCT)

(19) World Intellectual Property Organization
International Bureau

(43) International Publication Date
1 March 2012 (01.03.2012)

PCT

(10) International Publication Number
WO 2012/027203 A1

(51) International Patent Classification:
C09K 11/58 (2006.01) *C09K 11/88* (2006.01)

(21) International Application Number:
PCT/US2011/048299

(22) International Filing Date:
18 August 2011 (18.08.2011)

(25) Filing Language: English

(26) Publication Language: English

(30) Priority Data:
12/862,195 24 August 2010 (24.08.2010) US

(71) Applicant *(for all designated States except US)*: **MASSACHUSETTS INSTITUTE OF TECHNOLOGY** [US/US]; 77 Massachusetts Avenue, Cambridge, MA 02139-4307 (US).

(72) Inventors; and

(75) Inventors/Applicants *(for US only)*: **GREYTAK, Andrew, B.** [US/US]; 111 Waccamaw Avenue, Columbia, SC 29205 (US). **LIU, Wenhao** [US/US]; 70 Pacific Street, Cambridge, MA 02139 (US). **ALLEN, Peter, M.** [US/US]; 6 Marie Avenue #1, Cambridge, MA 02139 (US). **BAWENDI, Moungi, G.** [US/US]; 17 Lowell Street, Cambridge, MA 02138 (US). **NOCERA, Daniel, G.** [US/US]; 3 Bruce Road, Winchester, MA 01890 (US).

(74) Agents: **FOX, Harold, H.** et al.; STEPTOE & JOHNSON LLP, 1330 Connecticut Avenue, NW, Washington, DC 20036 (US).

(81) Designated States *(unless otherwise indicated, for every kind of national protection available)*: AE, AG, AL, AM, AO, AT, AU, AZ, BA, BB, BG, BH, BR, BW, BY, BZ, CA, CH, CL, CN, CO, CR, CU, CZ, DE, DK, DM, DO, DZ, EC, EE, EG, ES, FI, GB, GD, GE, GH, GM, GT,

[Continued on next page]

(54) Title: HIGHLY LUMINESCENT SEMICONDUCTOR NANOCRYSTALS

(57) Abstract: A semiconductor nanocrystal can have a photoluminescent quantum yield of at least 90%, at least 95%, or at least 98%. The nanocrystal can be made by sequentially contacting a nanocrystal core with an M-containing compound and an X donor, where at least one of the M-containing compound and the X donor is substoichiometric with respect to forming a monolayer on the nanocrystal core.

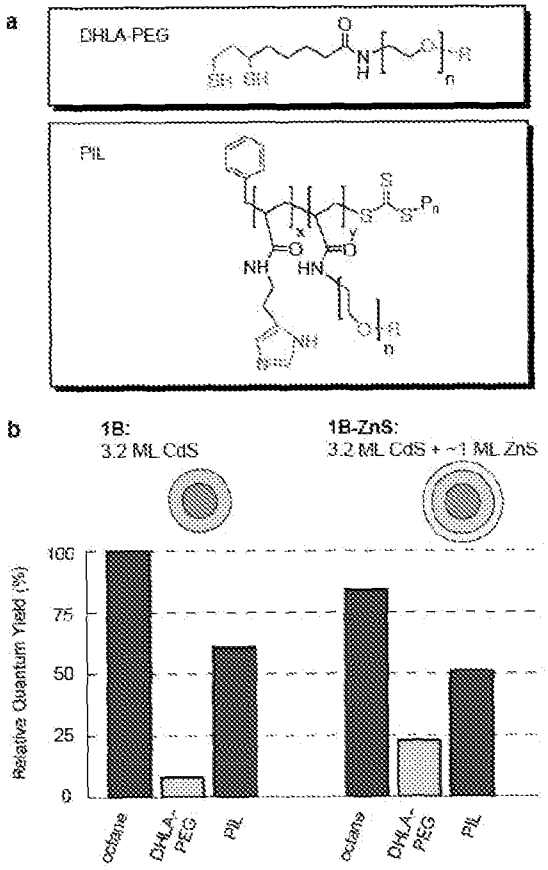

FIG. 4

WO 2012/027203 A1

HN, HR, HU, ID, IL, IN, IS, JP, KE, KG, KM, KN, KP, KR, KZ, LA, LC, LK, LR, LS, LT, LU, LY, MA, MD, ME, MG, MK, MN, MW, MX, MY, MZ, NA, NG, NI, NO, NZ, OM, PE, PG, PH, PL, PT, QA, RO, RS, RU, SC, SD, SE, SG, SK, SL, SM, ST, SV, SY, TH, TJ, TM, TN, TR, TT, TZ, UA, UG, US, UZ, VC, VN, ZA, ZM, ZW.

(84) Designated States *(unless otherwise indicated, for every kind of regional protection available)*: ARIPO (BW, GH, GM, KE, LR, LS, MW, MZ, NA, SD, SL, SZ, TZ, UG, ZM, ZW), Eurasian (AM, AZ, BY, KG, KZ, MD, RU, TJ, TM), European (AL, AT, BE, BG, CH, CY, CZ, DE, DK, EE, ES, FI, FR, GB, GR, HR, HU, IE, IS, IT, LT, LU, LV, MC, MK, MT, NL, NO, PL, PT, RO, RS, SE, SI, SK, SM, TR), OAPI (BF, BJ, CF, CG, CI, CM, GA, GN, GQ, GW, ML, MR, NE, SN, TD, TG).

Published:

— *with international search report (Art. 21(3))*

HIGHLY LUMINESCENT SEMICONDUCTOR NANOCRYSTALS

CLAIM OF PRIORITY

This application claims priority to U.S. Patent Application No. 12/862,195, filed August 24, 2010, which is incorporated by reference in its entirety.

FEDERALLY SPONSORED RESEARCH

This invention was made with government support under Grant No. R01 CA126642, awarded by the National Institute of Health and under Grant No. W911NF-06-1-0101, awarded by the Army Research Office. The government has certain rights in this invention.

FIELD OF THE INVENTION

This invention relates to highly luminescent semiconductor nanocrystals.

BACKGROUND

Semiconductor nanocrystals are a powerful class of nanostructures that exhibit high photoluminescence quantum yields, large molar extinction coefficients, high photostability compared to typical molecular fluorophores, and size-tunable emission wavelengths that can extend across the visible and near-IR spectral range. These properties make semiconductor nanocrystals useful in applications including biological fluorescent tags and light-emitting devices, among others.

SUMMARY

Semiconductor nanocrystals have size-dependent optical and electronic properties. In particular, the band gap energy of a semiconductor nanocrystal of a particular semiconductor material varies with the diameter of the crystal. Generally, a semiconductor nanocrystal is a member of a population of nanocrystals having a distribution of sizes. When the distribution is centered about a single value and narrow, the population can be described as monodisperse. Monodisperse particles can be defined as having at least 60% of the particles fall within a specified particle size range.

Monodisperse particles can deviate less in their diameters less than 10% rms and preferably less than 5% rms.

Many applications of semiconductor nanocrystals depend on their photoluminescent properties. Accordingly, semiconductor nanocrystals having narrow emission linewidths (expressed, for example, as a full width at half max) and high quantum yields are desirable.

In one aspect, a semiconductor nanocrystal can have a photoluminescent quantum yield of at least 90%. The photoluminescent quantum yield can be determined as a relative quantum yield or as an absolute quantum yield. The semiconductor nanocrystal can include a core including a first semiconductor material and a shell including a second semiconductor material.

The first semiconductor material can be ZnS, ZnSe, ZnTe, CdS, CdSe, CdTe, HgS, HgSe, HgTe, AlN, AlP, AlAs, AlSb, GaN, GaP, GaAs, GaSb, GaSe, InN, InP, InAs, InSb, TlN, TlP, TlAs, TlSb, PbS, PbSe, PbTe, or a mixture thereof. Independently, the second semiconductor material can be ZnS, ZnSe, ZnTe, CdS, CdSe, CdTe, HgS, HgSe, HgTe, AlN, AlP, AlAs, AlSb, GaN, GaP, GaAs, GaSb, GaSe, InN, InP, InAs, InSb, TlN, TlP, TlAs, TlSb, PbS, PbSe, PbTe, or a mixture thereof.

The semiconductor nanocrystal can be a member of a population of semiconductor nanocrystals, wherein the population exhibits photoluminescence with a full width at half max of less than 30 nm. In some embodiments, the first semiconductor material can be CdSe; independently, the second semiconductor material can be CdS.

In another aspect, a method of making a semiconductor nanocrystal includes forming a nanocrystal core including a first semiconductor material, and sequentially contacting the nanocrystal core with an M-containing compound and an X donor, thereby forming a second semiconductor material on a surface of the nanocrystal core, where at least one of the M-containing compound and the X donor is substoichiometric with respect to forming a monolayer on the nanocrystal core.

The method can include repeating the step of sequentially contacting the nanocrystal core with an M-containing compound and an X donor. Both the M-containing compound and the X donor can be substoichiometric with respect to forming a monolayer on the nanocrystal core. The M-containing compound can be selected to react quantitatively. The X donor can be selected to react quantitatively.

In the method, the first semiconductor material can be ZnS, ZnSe, ZnTe, CdS, CdSe, CdTe, HgS, HgSe, HgTe, AlN, AlP, AlAs, AlSb, GaN, GaP, GaAs, GaSb, GaSe, InN, InP, InAs, InSb, TlN, TlP, TlAs, TlSb, PbS, PbSe, PbTe, or a mixture thereof. Independently, the second semiconductor material can be ZnS, ZnSe, ZnTe, CdS, CdSe, CdTe, HgS, HgSe, HgTe, AlN, AlP, AlAs, AlSb, GaN, GaP, GaAs, GaSb, GaSe, InN, InP, InAs, InSb, TlN, TlP, TlAs, TlSb, PbS, PbSe, PbTe, or a mixture thereof.

In some embodiments, the first semiconductor material can be CdSe; independently, the second semiconductor material can be CdS. The X donor can be bis(trimethylsilyl)sulfide.

In another aspect, a population of semiconductor nanocrystals can exhibit photoluminescence with a quantum yield of at least 90% and a full width at half max (FWHM) of less than 30 nm. The population can exhibits photoluminescence with a quantum yield of at least 95%, or at least 98%.

Other embodiments are within the scope of the claims.

BRIEF DESCRIPTION OF THE DRAWINGS

FIGS. 1A-1C are graphs depicting optical properties of semiconductor nanocrystals with varying degrees of overcoating.

FIG. 2A is a TEM image of semiconductor nanocrystals. FIG. 2B is a histogram of semiconductor nanocrystal sizes.

FIG. 3 is a graph depicting WDS results for semiconductor nanocrystals.

FIG. 4A illustrates the general structure of hydrophilic ligands. FIG. 4B is a graph showing the effect of ZnS shell growth and ligand exchange on relative QY of CdSe/CdS core/shell nanocrystals. The relative QY is with reference to sample 1B diluted in octane; the absolute QY of this sample was >95%.

FIG. 5A shows time-resolved PL decay of nanocrystals in hexane solution. FIG. 5B is a decay trace obtained by integrating from 550 to 570 nm (thin black line). Monoexponential fit with τ_D = 26 ns (thick blue line).

FIG. 6 illustrates PL decay of nanocrystals in hexane excited with 400 nm light. Average pulse energy densities were (FIGS. 6A, 6B, and 6C) 7.7, 55, and 230 $\mu J/cm^2$, corresponding to average excitation densities $n \approx 0.07$, 0.5, and 2, respectively. (d) Decay of intensity integrated over a 550-570 nm window for the results shown in FIGS. 6A, 6B, and 6C.

FIGS. 7A-7D show blinking behavior of nanocrystals (570 nm emission peak, FIGS. 7A and 7B; and 610 nm emission peak, FIGS. 7C and 7D) under 514 nm CW excitation. FIGS. 7A and 7C: Left: Intensity traces for representative nanocrystals. Right: Distribution of intensities observed over time for these individual nanocrystals. The dashed line indicates the value chosen to demark "on" and "off" states in calculating the on-time fraction. On-time fractions for FIGS. 7A and 7C were 90% and 93%, respectively. FIGS. 7B and 7D are histograms indicating the distribution of on-time fractions among nanocrystals observed in each sample. The total number of nanocrystals observed was 56 and 45 in FIG. 7B and FIG. 7D, respectively.

DETAILED DESCRIPTION

Semiconductor nanocrystals demonstrate quantum confinement effects in their luminescent properties. When semiconductor nanocrystals are illuminated with a primary energy source, a secondary emission of energy occurs at a frequency that relates to the band gap of the semiconductor material used in the nanocrystal. In quantum confined particles, the frequency is also related to the size of the nanocrystal.

Core-shell heterostructures have been widely explored as a means to adjust the photophysical properties of semiconductor nanocrystals, and can be used to increase their brightness as fluorophores in two ways: (1) maximizing the photoluminescence (PL) quantum yield (QY) through electronic and chemical isolation of the core from surface-associated recombination centers; and (2) increasing the excitation rate (absorption cross-section) by building a high density of electronic states at energies above the shell bandgap. These two roles for the shell present a potential trade-off in terms of shell material. A wide bandgap shell imposes large electronic barriers for carrier access to the surface but will be less able to contribute to absorption, while a narrower gap shell could participate in light harvesting but may make it harder to achieve high QY.

For the case of CdSe, one of the best studied nanocrystal core materials, CdS and ZnS are isostructural materials that have been applied to form shells, both as pure materials and in heterostructures with alloyed and/or graded compositions of $Cd_xZn_{1-x}S$. The use of Cd-rich or pure CdS shells imposes challenges in maintaining high QY, and in terms of the strong redshift of the nanocrystal excited states encountered upon overcoating with a weakly-confining shell. The redshift imposes a strong requirement of

structural homogeneity in shell growth if inhomogeneous broadening of the PL emission spectrum is to be avoided.

In general, the method of manufacturing a nanocrystal is a colloidal growth process. See, for example, U.S. Patent Nos. 6,322,901 and 6,576,291, each of which is incorporated by reference in its entirety. Colloidal growth can result when an M-containing compound and an X donor are rapidly injected into a hot coordinating solvent. The coordinating solvent can include an amine. The M-containing compound can be a metal, an M-containing salt, or an M-containing organometallic compound. The injection produces a nucleus that can be grown in a controlled manner to form a nanocrystal. The reaction mixture can be gently heated to grow and anneal the nanocrystal. Both the average size and the size distribution of the nanocrystals in a sample are dependent on the growth temperature. The growth temperature necessary to maintain steady growth increases with increasing average crystal size. The nanocrystal is a member of a population of nanocrystals. As a result of the discrete nucleation and controlled growth, the population of nanocrystals obtained has a narrow, monodisperse distribution of diameters. The monodisperse distribution of diameters can also be referred to as a size. The process of controlled growth and annealing of the nanocrystals in the coordinating solvent that follows nucleation can also result in uniform surface derivatization and regular core structures. As the size distribution sharpens, the temperature can be raised to maintain steady growth. By adding more M-containing compound or X donor, the growth period can be shortened.

The M-containing salt can be a non-organometallic compound, e.g., a compound free of metal-carbon bonds. M can be cadmium, zinc, magnesium, mercury, aluminum, gallium, indium, thallium, or lead. The M-containing salt can be a metal halide, metal carboxylate, metal carbonate, metal hydroxide, metal oxide, or metal diketonate, such as a metal acetylacetonate. The M-containing salt is less expensive and safer to use than organometallic compounds, such as metal alkyls. For example, the M-containing salts are stable in air, whereas metal alkyls are generally unstable in air. M-containing salts such as 2,4-pentanedionate (i.e., acetylacetonate (acac)), halide, carboxylate, hydroxide, oxide, or carbonate salts are stable in air and allow nanocrystals to be manufactured under less rigorous conditions than corresponding metal alkyls.

Suitable M-containing salts include cadmium acetylacetonate, cadmium iodide, cadmium bromide, cadmium chloride, cadmium hydroxide, cadmium carbonate,

cadmium acetate, cadmium oxide, zinc acetylacetonate, zinc iodide, zinc bromide, zinc chloride, zinc hydroxide, zinc carbonate, zinc acetate, zinc oxide, magnesium acetylacetonate, magnesium iodide, magnesium bromide, magnesium chloride, magnesium hydroxide, magnesium carbonate, magnesium acetate, magnesium oxide, mercury acetylacetonate, mercury iodide, mercury bromide, mercury chloride, mercury hydroxide, mercury carbonate, mercury acetate, aluminum acetylacetonate, aluminum iodide, aluminum bromide, aluminum chloride, aluminum hydroxide, aluminum carbonate, aluminum acetate, gallium acetylacetonate, gallium iodide, gallium bromide, gallium chloride, gallium hydroxide, gallium carbonate, gallium acetate, indium acetylacetonate, indium iodide, indium bromide, indium chloride, indium hydroxide, indium carbonate, indium acetate, thallium acetylacetonate, thallium iodide, thallium bromide, thallium chloride, thallium hydroxide, thallium carbonate, or thallium acetate.

Alkyl is a branched or unbranched saturated hydrocarbon group of 1 to 100 carbon atoms, preferably 1 to 30 carbon atoms, such as methyl, ethyl, n-propyl, isopropyl, n-butyl, isobutyl, t-butyl, octyl, decyl, tetradecyl, hexadecyl, eicosyl, tetracosyl and the like, as well as cycloalkyl groups such as cyclopentyl, cyclohexyl and the like. Optionally, an alkyl can contain 1 to 6 linkages selected from the group consisting of -O-, -S-, -M- and -NR- where R is hydrogen, or C_1-C_8 alkyl or lower alkenyl.

Prior to combining the M-containing salt with the X donor, the M-containing salt can be contacted with a coordinating solvent to form an M-containing precursor. Typical coordinating solvents include alkyl phosphines, alkyl phosphine oxides, alkyl phosphonic acids, or alkyl phosphinic acids; however, other coordinating solvents, such as pyridines, furans, and amines may also be suitable for the nanocrystal production. Examples of suitable coordinating solvents include pyridine, tri-n-octyl phosphine (TOP) and tri-n-octyl phosphine oxide (TOPO). Technical grade TOPO can be used. The coordinating solvent can include a 1,2-diol or an aldehyde. The 1,2-diol or aldehyde can facilitate reaction between the M-containing salt and the X donor and improve the growth process and the quality of the nanocrystal obtained in the process. The 1,2-diol or aldehyde can be a C_6-C_{20} 1,2-diol or a C_6-C_{20} aldehyde. A suitable 1,2-diol is 1,2-hexadecanediol or myristol and a suitable aldehyde is dodecanal is myristic aldehyde.

The X donor is a compound capable of reacting with the M-containing salt to form a material with the general formula MX. Typically, the X donor is a chalcogenide donor or a pnictide donor, such as a phosphine chalcogenide, a bis(silyl) chalcogenide,

dioxygen, an ammonium salt, or a tris(silyl) pnictide. Suitable X donors include dioxygen, elemental sulfur, bis(trimethylsilyl) selenide ($(TMS)_2Se$), trialkyl phosphine selenides such as (tri-n-octylphosphine) selenide (TOPSe) or (tri-n-butylphosphine) selenide (TBPSe), trialkyl phosphine tellurides such as (tri-n-octylphosphine) telluride (TOPTe) or hexapropylphosphorustriamide telluride (HPPTTe), bis(trimethylsilyl)telluride ($(TMS)_2Te$), sulfur, bis(trimethylsilyl)sulfide ($(TMS)_2S$), a trialkyl phosphine sulfide such as (tri-n-octylphosphine) sulfide (TOPS), tris(dimethylamino) arsine, an ammonium salt such as an ammonium halide (e.g., NH_4Cl), tris(trimethylsilyl) phosphide ($(TMS)_3P$), tris(trimethylsilyl) arsenide ($(TMS)_3As$), or tris(trimethylsilyl) antimonide ($(TMS)_3Sb$). In certain embodiments, the M donor and the X donor can be moieties within the same molecule.

The nanocrystal manufactured from an M-containing salt grows in a controlled manner when the coordinating solvent includes an amine. The amine in the coordinating solvent can contribute to the quality of the nanocrystal obtained from the M-containing salt and X donor. Preferably, the coordinating solvent is a mixture of the amine and an alkyl phosphine oxide. The combined solvent can decrease size dispersion and can improve photoluminescence quantum yield of the nanocrystal. The preferred amine is a primary alkyl amine or a primary alkenyl amine, such as a C_2-C_{20} alkyl amine, a C_2-C_{20} alkenyl amine, preferably a C_8-C_{18} alkyl amine or a C_8-C_{18} alkenyl amine. For example, suitable amines for combining with tri-octylphosphine oxide (TOPO) include l-hexadecylamine, or oleylamine. When the 1,2-diol or aldehyde and the amine are used in combination with the M-containing salt to form a population of nanocrystals, the photoluminescence quantum efficiency and the distribution of nanocrystal sizes are improved in comparison to nanocrystals manufactured without the 1,2-diol or aldehyde or the amine.

The nanocrystal can be a member of a population of nanocrystals having a narrow size distribution. The nanocrystal can be a sphere, rod, disk, or other shape. The nanocrystal can include a core of a semiconductor material. The nanocrystal can include a core having the formula MX, where M is cadmium, zinc, magnesium, mercury, aluminum, gallium, indium, thallium, or mixtures thereof, and X is oxygen, sulfur, selenium, tellurium, nitrogen, phosphorus, arsenic, antimony, or mixtures thereof.

The emission from the nanocrystal can be a narrow Gaussian emission band that can be tuned through the complete wavelength range of the ultraviolet, visible, or infrared

regions of the spectrum by varying the size of the nanocrystal, the composition of the nanocrystal, or both. For example, both CdSe and CdS can be tuned in the visible region and InAs can be tuned in the infrared region.

A population of nanocrystals can have a narrow size distribution. The population can be monodisperse and can exhibit less than a 15% rms deviation in diameter of the nanocrystals, preferably less than 10%, more preferably less than 5%. Spectral emissions in a narrow range of between 10 and 100 nm full width at half max (FWHM) can be observed. Semiconductor nanocrystals can have emission quantum efficiencies (i.e., quantum yields, QY) of greater than 2%, 5%, 10%, 20%, 40%, 60%, 70%, 80%, or 90%. Semiconductor nanocrystals can have a QY of at least 90%, at least 91%, at least 92%, at least 93%, at least 94%, at least 95%, at least 96%, at least 97%, at least 97%, at least 98%, or at least 99%.

The semiconductor forming the core of the nanocrystal can include Group II-VI compounds, Group II-V compounds, Group III-VI compounds, Group III-V compounds, Group IV-VI compounds, Group I-III-VI compounds, Group II-IV-VI compounds, and Group II-IV-V compounds, for example, ZnS, ZnSe, ZnTe, CdS, CdSe, CdTe, HgS, HgSe, HgTe, AlN, AlP, AlAs, AlSb, GaN, GaP, GaAs, GaSb, GaSe, InN, InP, InAs, InSb, TlN, TlP, TlAs, TlSb, PbS, PbSe, PbTe, or mixtures thereof.

The quantum efficiency of emission from nanocrystals having a core of a first semiconductor material can be enhanced by applying an overcoating of a second semiconductor material such that the conduction band of the second semiconductor material is of higher energy than that of the first semiconductor material, and the valence band of the second semiconductor material is of lower energy than that of the first semiconductor material. As a result, charge carriers, i.e., electrons and holes, are confined in the core of the nanocrystal when in an excited state. Alternatively, the conduction band or valence band of overcoating material can have an energy intermediate between the energies of the conduction and valence bands of the core material. In this case, one carrier can be confined to the core while the other is confined to the overcoating material when in an excited state. See, for example, U.S. Patent No. 7,390,568, which is incorporated by reference in its entirety. The core can have an overcoating on a surface of the core. The band gap of core and overcoating can have a desired band offset. In CdTe/CdSe (core/shell) nanocrystals, the conduction band of the shell is intermediate in energy to the valence band and conduction band of the core. CdTe/CdSe (core/shell)

nanocrystals have lower potentials for the holes in the core and for the electrons in the shell. As a result, the holes can be mostly confined to the CdTe core, while the electrons can be mostly confined to the CdSe shell. CdSe/ZnTe (core/shell) nanocrystals have the valence band of the shell intermediate in energy to the valence band and conduction band of the core. As a result, the electrons reside mostly in the CdSe cores, while the holes reside mostly in the ZnTe shells. The overcoating can be a semiconductor material having a composition different from the composition of the core, and can have a band gap greater than the band gap of the core. The overcoat of a semiconductor material on a surface of the nanocrystal can include a Group II-VI compounds, Group II-V compounds, Group III-VI compounds, Group III-V compounds, Group IV-VI compounds, Group I-III-VI compounds, Group II-IV-VI compounds, and Group II-IV-V compounds, for example, ZnS, ZnSe, ZnTe, CdS, CdSe, CdTe, HgS, HgSe, HgTe, AlN, AlP, AlAs, AlSb, GaN, GaP, GaAs, GaSb, GaSe, InN, InP, InAs, InSb, TlN, TlP, TlAs, TlSb, PbS, PbSe, PbTe, or mixtures thereof.

Shells are formed on nanocrystals by introducing shell precursors at a temperature where material adds to the surface of existing nanocrystals but at which nucleation of new particles is rejected. In order to help suppress nucleation and anisotropic elaboration of the nanocrystals, selective ionic layer adhesion and reaction (SILAR) growth techniques can be applied. See, e.g., U.S. Patent No. 7,767,260, which is incorporated by reference in its entirety. In the SILAR approach, metal and chalcogenide precursors are added separately, in an alternating fashion, in doses calculated to saturate the available binding sites on the nanocrystal surfaces, thus adding one-half monolayer with each dose. The goals of such an approach are to: (1) saturate available surface binding sites in each half-cycle in order to enforce isotropic shell growth; and (2) avoid the simultaneous presence of both precursors in solution so as to minimize the rate of homogenous nucleation of new nanoparticles of the shell material.

In the SILAR approach, it can be beneficial to select reagents that react cleanly and to completion at each step. In other words, the reagents selected should produce few or no reaction by-products, and substantially all of the reagent added should react to add shell material to the nanocrystals. Completion of the reaction can be favored by adding sub-stoichiometric amounts of the reagent. In other words, when less than one equivalent of the reagent is added, the likelihood of any unreacted starting material remaining is decreased.

Furthermore, the quality of core-shell nanocrystals produced (e.g., in terms of size monodispersity and QY) can be enhanced by using a constant and lower shell growth temperature than has been typically been used in the past. Alternatively, high temperatures may also be used. The techniques described here are amenable to a wide temperature range, unlike earlier SILAR methods that worked only at very high temperatures. In addition, a low-temperature or room temperature "hold" step can be used during the synthesis or purification of core materials prior to shell growth.

The outer surface of the nanocrystal can include a layer of compounds derived from the coordinating agent used during the growth process. The surface can be modified by repeated exposure to an excess of a competing coordinating group to form an overlayer. For example, a dispersion of the capped nanocrystal can be treated with a coordinating organic compound, such as pyridine, to produce crystals which disperse readily in pyridine, methanol, and aromatics but no longer disperse in aliphatic solvents. Such a surface exchange process can be carried out with any compound capable of coordinating to or bonding with the outer surface of the nanocrystal, including, for example, phosphines, thiols, amines and phosphates. The nanocrystal can be exposed to short chain polymers which exhibit an affinity for the surface and which terminate in a moiety having an affinity for a suspension or dispersion medium. Such affinity improves the stability of the suspension and discourages flocculation of the nanocrystal.

Monodentate alkyl phosphines (and phosphine oxides; the term phosphine below will refer to both) can passivate nanocrystals efficiently. When nanocrystals with conventional monodentate ligands are diluted or embedded in a non-passivating environment (i.e., one where no excess ligands are present), they tend to lose their high luminescence. Typical are an abrupt decay of luminescence, aggregation, and/or phase separation. In order to overcome these limitations, polydentate ligands can be used, such as a family of polydentate oligomerized phosphine ligands. The polydentate ligands show a high affinity between ligand and nanocrystal surface. In other words, they are stronger ligands, as is expected from the chelate effect of their polydentate characteristics.

In general, a ligand for a nanocrystal can include a first monomer unit including a first moiety having affinity for a surface of the nanocrystal, a second monomer unit including a second moiety having a high water solubility, and a third monomer unit including a third moiety having a selectively reactive functional group or a selectively binding functional group. In this context, a "monomer unit" is a portion of a polymer

derived from a single molecule of a monomer. For example, a monomer unit of poly(ethylene) is $-CH_2CH_2-$, and a monomer unit of poly(propylene) is $-CH_2CH(CH_3)-$. A "monomer" refers to the compound itself, prior to polymerization, e.g., ethylene is a monomer of poly(ethylene) and propylene of poly(propylene).

A selectively reactive functional group is one that can form a covalent bond with a selected reagent under selected conditions. One example of a selectively reactive functional group is a primary amine, which can react with, for example, a succinimidyl ester in water to form an amide bond. A selectively binding functional group is a functional group that can form a noncovalent complex with a selective binding counterpart. Some well known examples of selectively binding functional groups and their counterparts include biotin and streptavidin; a nucleic acid and a sequence-complementary nucleic acid; FK506 and FKBP; or an antibody and its corresponding antigen.

A moiety having high water solubility typically includes one or more ionized, ionizable, or hydrogen bonding groups, such as, for example, an amine, an alcohol, a carboxylic acid, an amide, an alkyl ether, a thiol, or other groups known in the art. Moieties that do not have high water solubility include, for example, hydrocarbyl groups such as alkyl groups or aryl groups, haloalkyl groups, and the like. High water solubility can be achieved by using multiple instances of a slightly soluble group: for example, diethyl ether is not highly water soluble, but a poly(ethylene glycol) having multiple instances of a $-CH_2-O-CH_2-$ alkyl ether group can be highly water soluble.

For example, the ligand can include a polymer including a random copolymer. The random copolymer can be made using any method of polymerization, including cationic, anion, radical, metathesis or condensation polymerization, for example, living cationic polymerization, living anionic polymerization, ring opening metathesis polymerization, group transfer polymerization, free radical living polymerization, living Ziegler-Natta polymerization, or reversible addition fragmentation chain transfer (RAFT) polymerization.

EXAMPLES

Cadmium selenide nanocrystal cores were synthesized using cadmium oxide and trioctylphosphine selenide precursors in the presence of tetradecylphosphonic acid (TDPA) in a solvent of trioctylphosphine (TOP) and trioctylphosphine oxide (TOPO).

See, e.g., Murray, C.; et al. *Journal of the American Chemical Society* **1993**, *115*, 8706-8715, which is incorporated by reference in its entirety. Care was required in isolating core nanocrystals from byproducts of the core synthesis reaction in order to avoid nucleation of CdS particles in subsequent overcoating steps. CdSe cores were isolated by two cycles of flocculation from hexane with acetone, holding the nanocrystals in pure hexane solution at 4 °C overnight between cycles and decanting the nanocrystal solution from precipitates that appeared.

Growth of conformal CdS shells (overcoating) on the CdSe nanocrystal cores was accomplished at a constant temperature (typically 180 °C) in a solvent of oleylamine and 1-octadecene (ODE). The cadmium precursor was Cd oleate in a solvent of 50:50 ODE and TOP with two equivalents of decylamine (vs. Cd) added. The sulfur precursor was hexamethyldisilathiane (TMS_2S) in TOP (see, for example, Hines, M.; Guyot-Sionnest, P. *Journal of Physical Chemistry* **1996**, *100*, 468-471; Kuno, M.; et al. *Journal of Chemical Physics* **1997**, *106*, 9869-9882; and Snee, P.; et al. *Advanced Materials* **2005**, *17*, 1131; each of which is incorporated by reference in its entirety. This is in contrast to most nanocrystal SILAR literature, in which a preparation of elemental S in olefin solvents has been used. See, e.g., Li, J.; et al. *J. Am. Chem. Soc.* **2003**, *125*, 12567-12575; Xie, R.; et al. *J. Am. Chem. Soc.* **2005**, *127*, 7480-7488; Chen, Y.; et al. *J. Am. Chem. Soc.* **2008**, *130*, 5026-5027; van Embden, J.; et al. *Journal of the American Chemical Society* **2009**; Mahler, B.; et al. *Nat Mater* **2008**, *7*, 659-664; and Jha, P. P.; Guyot-Sionnest, P. *ACS Nano* **2009**, *3*, 1011-1015; each of which is incorporated by reference in its entirety.

Cadmium and sulfur precursors were added alternately in doses calculated to provide slightly less than one monolayer (ML) of surface coverage. The marginal thickness of one ML is taken as ½ of the c-axis lattice constant for CdS with the wurtzite crystal structure, or 0.337 nm (Xie, R.; et al. *J. Am. Chem. Soc.* **2005**, *127*, 7480-7488; and Kuno, M.; et al. *Journal of Chemical Physics* **1997**, *106*, 9869-9882; each of which is incorporated by reference in its entirety). The volume of such a shell was divided by the CdS unit cell volume to determine the quantity of precursor that was required for each dose. The quantity (number of moles) of CdSe cores in a given preparation and the core radius were determined by estimating the molar extinction coefficient of the core batch on the basis of the wavelength of the lowest-energy absorption feature (see, for example, Leatherdale, C.; et al. *Journal of Physical Chemistry B* **2002**, *106*, 7619-7622, which is incorporated by reference in its entirety). The waiting time was 15 min between the start

of each addition, and the precursor doses were added by syringe pump over a 3 minute injection time. Following shell growth, the solution was quantitatively recovered. The progress and yield of the overcoating reaction were monitored via UV-VIS absorption, PL, and transmission electron microscopy (TEM), and wavelength dispersive spectroscopy (WDS) compositional analysis.

Samples showed striking increases in brightness under room light upon overcoating with CdS. The PL QY was measured using an integrating sphere under 514 nm excitation, and found to be 98% for the sample described in Example 2. Characteristic values fell between 90% and 98%. Table 1 summarizes results from literature and from the present work.

Table 1.

Core radius	Shell thickness	Method	Ensemble QY	Ref
	CdS shell			
1.3 nm	1.3 nm	SILAR[a]	98%	This work
1.2	0.7	Simultaneous[d]	50-100%[f]	Peng et al.[12]
1.7	1.7	SILAR[b]	40%	Li et al.[18]
1.6	1.4	SILAR[b]	65%	Xie et al.[17]
2	6	SILAR[b]	40%	Chen et al.[15]
2	< 6	SILAR[b]	Up to 90%	Chen et al.[15]
2.5	4	SILAR[b]	70%	Mahler et al.[20]
1.3	2.2	SILAR[b]	70%[c]	van Embden et al.[21]
	ZnS or CdZnS shell			
1.5	0.6 ZnS	Simultaneous[d]	50%	Hines & Guyot-Sionnest[11]
2.1	0.4 ZnS	Simultaneous[d]	50%	Dabbousi et al.[13]
6	1-5[e]	Commercial (QDC)	100%	McBride et al.[19]
1.6	1 (graded CdS/ZnS)	SILAR	80%	Xie et al.[17]

a. TMS_2S sulfur precursor

b. ODE/S sulfur precursor

c. Activated with addition of trioctylphosphine and octadecylamine

d. Using Et_2Zn or Me_2Cd and TMS_2S

e. Highly anisotropic shell coverage

f. Relative QYs; sample-to-sample variation reported.

g. References (each of which is incorporated by reference in its entirety): Peng, X., et al., *J. Am. Chem. Soc.* **1997**, *119*, 7019-7029; Li, J. J., et al., *J. Am. Chem. Soc.* **2003**, *125*, 12567-12575; Xie, R., et al., *J. Am. Chem. Soc.* **2005**, *127*, 7480-7488; Chen, Y., et al., *J. Am. Chem. Soc.* **2008**, *130*, 5026-5027; Mahler, B., et al., *Nat Mater* **2008**, *7*, 659-664; van Embden, J., et al., *J. Am. Chem. Soc.* **2009**, *131*,

14200-14309; Hines, M. A. and Guyot-Sionnest, P., *J. Phys. Chem.* **1996**, *100*, 468-471; Dabbousi, B. O., et al., *J. Phys. Chem. B* **1997**, *101*, 9463-9475; and McBride, J., et al., *Nano Letters* **2006**, *6*, 1496-1501.

Core-shell nanocrystal heterostructures have been explored widely as a means to adjust the photophysical properties of nanocrystals, (see, e.g., Hines, M.; Guyot-Sionnest, P. *Journal of Physical Chemistry* **1996**, *100*, 468-471; and Ivanov, S.; Piryatinski, A.; Nanda, J.; Tretiak, S.; Zavadil, K.; Wallace, W.; Werder, D.; Klimov, V. Type-II Core/Shell CdS/ZnSe Nanocrystals: Synthesis, Electronic Structures, and Spectroscopic Properties. *J. Am. Chem. Soc.* **2007**, each of which is incorporated by reference in its entirety) and can be used to increase their brightness as fluorophores in two ways: (1) maximizing the PL QY through electronic and chemical isolation of the core from surface-associated recombination centers; and (2) increasing the excitation rate (absorption cross-section) by building a high density of electronic states at energies above the shell bandgap. These two roles for the shell present a potential trade-off in terms of shell material. A wide bandgap shell imposes large electronic barriers for carrier access to the surface but will be less able to contribute to absorption, while a narrower gap shell could participate in light harvesting but may make it harder to achieve high QY.

For the case of CdSe, one of the best studied nanocrystal nanocrystal core materials, the sulfides of zinc and cadmium (ZnS and CdS) are isostructural materials that have been applied to form shells, both as pure materials and in heterostructures with alloyed and/or graded compositions of $Cd_xZn_{1-x}S$. See, for example, Xie, R.; et al. *J. Am. Chem. Soc.* **2005**, *127*, 7480-7488; Hines, M.; Guyot-Sionnest, P. *Journal of Physical Chemistry* **1996**, *100*, 468-471; Kuno, M.; et al. *Journal of Chemical Physics* **1997**, *106*, 9869-9882; Snee, P.; et al. *Advanced Materials* **2005**, *17*, 1131; and Peng, X.; et al. *Journal of the American Chemical Society* **1997**, *119*, 7019-7029; each of which is incorporated by reference in its entirety. The use of Cd-rich or pure CdS shells imposes challenges in maintaining high QY (literature QY values are characteristically 20-65% for CdS shells of comparable thickness; see, e.g., Li, J.; et al. *J. Am. Chem. Soc.* **2003**, *125*, 12567-12575; Xie, R.; et al. *J. Am. Chem. Soc.* **2005**, *127*, 7480-7488; van Embden, J.; Jasieniak, J.; Mulvaney, P. Mapping the Optical Properties of CdSe/CdS Heterostructure Nanocrystals: The Effects of Core Size and Shell Thickness. *Journal of the American Chemical Society* **2009**; and Peng, X.; et al. *Journal of the American Chemical Society* **1997**, *119*, 7019-7029; each of which is incorporated by reference in its entirety) in terms

of the strong redshift of the nanocrystal excited states encountered upon overcoating with a weakly-confining shell. The redshift imposes a strong requirement of structural homogeneity in shell growth if inhomogeneous broadening of the PL emission spectrum is to be avoided.

Conformal shells on nanocrystals are generally produced by introducing shell precursors in a manner such that material adds to the surface of existing nanocrystals but nucleation of new particles is rejected. In order to help suppress nucleation and anisotropic elaboration of the nanocrystals, selective ionic layer adhesion and reaction (SILAR) growth techniques have been applied. In the SILAR approach, metal and chalcogenide precursors are added separately, in an alternating fashion. The goals of such an approach are to: (1) saturate available surface binding sites in each half-cycle in order to enforce isotropic shell growth; and (2) avoid the simultaneous presence of both precursors in solution so as to minimize the rate of homogenous nucleation of new nanoparticles of the shell material.

Among the features in the synthetic methods described here are: 1) the application of TMS_2S as a sulfur precursor in alternate-layer-addition shell growth; 2) the use of sub-monolayer reagent doses in each half-cycle; 3) the use of a constant, and lower, shell growth temperature than is characteristic; and 4) the use of a low-temperature "hold" step to aid in isolation of CdSe cores prior to CdS shell growth.

Salient features that make this an attractive synthetic procedure for scientific and commercial purposes include: 1) the achievement of high photoluminescence QY from CdSe nanocrystals with a shell of constant composition (CdS) and a high excitation rate at blue excitation wavelengths; 2) the avoidance of pyrophoric shell precursor materials (e.g. dimethylcadmium, which has been widely used); 3) the use of liquid-phase shell growth solvents, which aids recovery and further processing of overcoated nanocrystals; and 4) the quantitative conversion of shell growth reagents, which aids in programming of desired photoluminescence characteristics in the resulting particles and limits waste.

Ligand exchange of CdSe/CdS nanocrystals using a polymeric imidazole ligand (PIL) is described in detail below (Liu, W.; et al. *Journal of the American Chemical Society* **2010**, *132*, 472-483, which is incorporated by reference in its entirety). The resulting change in PL QY upon displacement of the native nanocrystal surface coating by the PIL and subsequent dissolution in water is shown. Importantly, the PIL system yields CdS-coated nanocrystals that retain QY of > 60% in aqueous solution. This is

comparable to or greater than the PL QY found for similar preparations using nanocrystals with ZnS- or CdZnS alloy-terminated shells. The hydrodynamic diameter (HD) of the resulting aqueous CdSe/CdS core/shell nanocrystals was ca. 11.5 nm. The nanocrystals described above are thus applicable as bright (high excitation rate, high PL QY) inorganic fluorophores in aqueous environments.

The alternate layer addition strategy described may be extended to core/shell material systems other than CdSe/CdS in cases where such is desirable. For example, while the PIL ligand exchange system works well with the pure CdS shell, ligand exchange with thiol-based hydrophilic coatings (Liu, W.; et al. *J. Am. Chem. Soc.* **2008**, *130*, 1274-1284, which is incorporated by reference in its entirety) can cause a significant decrease in QY. A thin ZnS shell can be applied to the surface of the CdSe/CdS QDs (creating a CdSe/CdS/ZnS core/shell/shell heterostructure) by substituting Zn oleate for Cd oleate in the synthetic procedure. This system experiences a significantly smaller decrease in QY on ligand exchange with thiols than does the CdSe/CdS system.

Materials: TOPO (99%), decylamine, ODE, oleic acid, and oleylamine were purchased from Aldrich. TOP, CdO, and Et_2Zn were purchased from Strem. Selenium and TMS_2S were purchased from Alfa Aesar. TOPSe (1.5 M) was prepared by dissolving Se in TOP. A stock solution of Cd oleate in ODE (0.2 M) was prepared by heating CdO in ODE with 2.1 eq. of oleic acid at 300 °C under nitrogen followed by degassing under vacuum at a lower temperature. DHLA-PEG and PIL ligands were prepared as described in Liu, W., et al., *J. Am. Chem. Soc.* 2008, 130, 1274-1284; and in Liu, W., et al. *J. Am. Chem. Soc.* 2010, 132, 472-483; each of which is incorporated by reference in its entirety.

Example 1: CdSe Core Synthesis. Cadmium selenide nanocrystal cores were synthesized in a solvent of equal parts trioctylphosphine (TOP) and trioctylphosphine oxide (TOPO). The Cd precursor was generated in situ by heating CdO with tetradecylphosphonic acid (TDPA) at 330 °C under flowing nitrogen until the solution became colorless. Following removal of evolved H_2O under vacuum at reduced temperature, the solution was heated to 360 °C under nitrogen. A solution of trioctylphosphine selenide (TOPSe) in TOP was rapidly introduced, and the system was allowed to react at ~300 °C for a short time before cooling to room temperature and storage as a yellow waxy solid. The batch used in the following example was prepared using a Se:TDPA:Cd ratio of 2.25:2:1 and exhibited a lowest-energy exciton absorption

feature at 487 nm, and showed a well-resolved band-edge photoluminescence peak, but low PL QY, when dispersed in hexanes.

Example 2: CdSe/CdS Core/Shell Synthesis. A portion of the crude CdSe core batch was warmed gently, diluted with hexanes, and centrifuged to remove any undissolved material. The nanocrystals were then flocculated by addition of acetone and/or methanol. After decanting the supernatant liquid, the nanocrystals were brought into hexanes and held as such at 4 °C for a period of 4-24 hours. This treatment caused precipitation of a colorless byproduct and was suppressed nucleation of CdS nanoparticles during subsequent shell growth. Then, the sample was again centrifuged and any precipitated material discarded prior to addition of a polar solvent to flocculate the nanocrystals a second time. After this, the nanocrystals were brought into a measured volume of hexane and their UV-VIS absorption spectrum was recorded at measured dilution to gauge the size and quantity of nanocrystals.

The nanocrystals were introduced to a solvent of 2:1 octadecene:oleylamine (v/v) and degassed at 100 °C to remove hexanes. The system was placed under nitrogen and heated to 180 °C before commencing reagent addition via syringe pump. Solution A (Cd precursor): to a solution of 0.2 M Cd oleate in octadecene was added 2 equivalents of decylamine, followed by a volume of TOP to yield a Cd concentration of 0.1 M. Solution B (S precursor) was a 0.1 M solution of TMS_2S in TOP. Alternating injections of Solutions A and B were performed, starting every 15 minutes. The injection flow rate was adjusted so that the desired dose for each cycle was added over the course of 3 minutes. At the conclusion of the reaction, the temperature was reduced to ambient, and the sample (a strongly colored and strongly fluorescent oil) was retrieved quantitatively and its total volume recorded to aid in calculation of the molar extinction coefficient.

FIGS. 1A-1C illustrate the shift in electronic spectra of CdSe nanocrystals upon CdS shell deposition by the described alternate layer addition approach. FIG. 1A: shift in absorption spectra for synthesis described in Example 2. Absorption spectra of CdSe nanocrystals (dark blue), and the same after 1 (green), 2 (red), 3 (light blue), 4 (purple), and 5 (yellow) complete addition cycles of CdS precursors. Spectra are normalized such that value at longest-wavelength absorption peak is 1. Inset: Absorption spectra of CdSe nanocrystals and 5-cycle-coated products presented in molar extinction units (liters / mole-cm). FIG. 1B, shift in PL emission spectrum for synthesis described in Example 2, under 365 nm excitation, with spectra normalized such that the peak value is 1, and with

traces colored to match those in FIG. 1A. FIG. 1C, absorption and emission spectrum peak energies versus predicted CdS shell thickness for the sample in Example 2 (marked **1A**), for a sample prepared similarly with only 4 cycles of CdS addition (marked **1B**), and for a sample prepared using larger (and lower-energy) CdSe nanocrystal starting material (marked **2**).

FIG. 2A shows a representative bright-field TEM image of nanoparticles (of Example 2) supported on carbon film. Scalebar, 20 nm. FIG. 2B, particle size analysis of the image in FIG. 2A, performed using NIH Image-J software, and revealing a mean radius of 2.76 nm. The shaded box represents the standard deviation of measured particle radii.

Elemental Analysis: Wavelength Dispersive Spectroscopy (WDS) was used to determine the elemental composition of the nanocrystal inorganic core. Dried nanocrystal samples were placed onto a silicon wafer and coated with amorphous carbon to prevent charging during measurements. Samples were then analyzed by WDS on a JEOL 733 scanning electron microscope (SEM).

FIG. 3 shows results of wavelength dispersive spectroscopy (WDS) analysis of the Cd, Se, and S elemental composition of CdSe/CdS core/shell nanocrystals. Dashed horizontal lines indicate measured ratios of Cd to Se (red) and Cd to S (green) for sample 1B described in FIG. 1C. Curves represent predicted elemental ratios for Cd to Se (red) and Cd to S (green) for concentric sphere and shell with bulk CdS and CdSe atomic densities as a function of the ratio of total radius (core + shell) to core radius alone. Crossing points with measured data provide an estimate of the shell thickness; the average of the Cd/Se and Cd/S curves is displayed as a broken vertical line. It shows relatively close agreement with the targeted shell thickness (dashed vertical line) that was used as the basis for CdS precursor doses.

Example 3: Quantum yield measurements. Absolute quantum yields were measured using an integrating sphere. See Popović, Z.; *Angew. Chemie Int. Ed.* 2010, 49, 8649-8652, which is incorporated by reference in its entirety. Laser excitation (514 nm) was chopped (80 Hz) and directed to an integrating sphere in which an NMR tube containing the sample (1 mL) was placed. Reference signals (i.e. solutions without emitting species) were also collected. Output light from the sphere was passed through a cutoff filter and collected on a photodetector (Newport 818 UV calibrated photodetector) generating a current intensity on a lock amplifier. The quantum yield value was obtained

by dividing a difference of sample and reference signals (with cutoff filter) with a difference of reference and sample signals without a cutoff filter. This method was verified by measuring quantum yields of standard laser dyes Rhodamine 101 and Rhodamine B in clear and scattering solutions (by addition of 100 nm diameter silica particles). The obtained values for laser dyes were: Rhodamine 101: 0.99 (ref: 1.00), Rhodamine B: 0.33 (ref: 0.31). See, e.g., Magde, D.; et al. *Photochemistry and Photobiology* **1999**, *70*, 737-744, which is incorporated by reference in its entirety.

For relative quantum yield measurements, fluorescence spectra of sample and reference were recorded using a BioTeK plate reader under 450 nm excitation. Measurements were conducted in triplicate and averaged. The optical density was kept below 0.1 between 400-800 nm, and the integrated intensities of the emission spectra, corrected for differences in optical density (measured at the excitation wavelength) and the solvent index of refraction, were used to calculate the quantum yields using the expression $QY_{QD} = QY_{Dye} \times (Absorbance_{dye} / Absorbance_{QD}) \times (Peak\ Area_{QD} / Peak\ Area_{Dye}) \times (n_{QD\ solvent})^2/(n_{Dye\ solvent})^2$.

Example 4: Ligand Exchange. CdSe/CdS core/shell nanocrystals (2 nmol) were flocculated from the stock solution using acetone and brought into 50 μL of chloroform ($CHCl_3$). The nanocrystal stock solution was mixed with a solution of PIL ligand (5 mg in 30 μL $CHCl_3$) that bore equimolar imidazole and methoxy-terminated oligo(ethylene glycol) sidechains. See, e.g., U.S. Patent Application No. 61/316,659, filed March 23, 2010, and PCT US2011/029492, filed March 23, 2011, each of which is incorporated by reference in its entirety. The mixture was stirred for 10 min at room temperature, after which 30 μL of methanol was added followed by stirring for an additional 20 min. At this time, the addition of EtOH (30 μL), $CHCl_3$ (30 μL), and excess hexanes brought about the flocculation of the nanocrystals. The sample was centrifuged. The clear supernatant was discarded, and the pellet dried in vacuo. The sample was then brought into aqueous solution by the addition of phosphate buffered saline (500 μL, pH 7.4).

FIG. 4B shows the change in PL QY of CdSe/CdS nanocrystals (sample 1B from FIG. 1C) upon surface ligand exchange as described in Example 4. Nanocrystals brought into neutral aqueous solution displayed 60% QY relative to the same dispersed in octane. The nanocrystals in octane were separately measured to have an absolute QY > 90%. The inset depicts the generalized structure of the polymeric imidazole ligand used: in the above, R = CH_3, n = 11, and x = y = 50%. P_n represents a second polymer chain nucleated

by the same trithiocarbonate reversible addition-fragmentation transfer (RAFT) polymerization reaction center. See, e.g., U.S. Patent Application No. 61/316,659, filed March 23, 2010, and PCT US2011/029492, filed March 23, 2011, each of which is incorporated by reference in its entirety.

FIG. 4A depicts two strategies that we have explored for bringing the hydrophobically capped nanocrystals described above into aqueous solution via ligand exchange, both as a means towards the use of these nanocrystals in biological imaging applications and as a way to explore the effect of different surface terminations on their photophysical properties – particularly the QY. The first system used PEGylated dihydrolipoic acid (DHLA-PEG) small-molecule ligands that were designed to coordinate the nanocrystal surface via the thiol groups. The second system used polymeric imidazole ligands (PILs): acrylic copolymers that were designed to chelate the nanocrystal surface via imidazole sidechains, in a manner analogous to poly-histidine peptide domains[33] and PEGylated sidechains that provide water solubility (see, e.g., Goldman, E. R. et al., *Analytica Chimica Acta* 2005, 534, 63-67, which is incorporated by reference in its entirety).

Samples **1B** and **1B-ZnS** were ligand exchanged with DHLA-PEG (PEG8, 80% hydroxyl terminated, 20% amine-terminated) and PIL ligands (a random copolymer of 50% methoxy-PEG-11, 50% imidazole sidechains) as described previously, yielding well-dispersed aqueous solutions. The absorption and fluorescence lineshapes of the ligand exchanged nanocrystals were essentially unchanged. Dilute solutions of the resulting hydrophilic nanocrystals were prepared in phosphate buffered saline (PBS) for quantum yield measurements.

FIG. 4B displays the relative quantum yield of these samples, using sample **1B** diluted in octane as the reference (absolute QY >95%). The CdSe/CdS core/shell nanocrystals experienced a dramatic quench of their relative PL QY to just 8% upon ligand exchange with thiol-bearing DHLA-PEG. While even a single thiol ligand can cause a measurable quench of CdSe nanocrystal fluorescence, (see, e.g., Munro, A.M., and Ginger, D.S., *Nano Lett.* **2008**, *8*, 2585-2590, which is incorporated by reference in its entirety) we have previously shown that the DHLA-PEG ligand yielded aqueous absolute QYs of 30-40% when used on CdSe/$Cd_{0.2}Zn_{0.8}S$ core/shell nanocrystals of several monolayer shell thickness. Indeed, the addition of the ZnS shell to form CdSe/CdS/ZnS nanocrystals was able to rescue the QY of DHLA-PEG coated

nanocrystals substantially, even though the addition of the ZnS caused a decrease in the relative QY of the starting hydrophobically-coated nanocrystals to 84% versus the CdSe/CdS reference. A remarkably different result was found when the nanocrystals were cap exchanged with the imidazole-bearing PIL ligand. Aqueous PIL-coated CdSe/CdS nanocrystals maintained a relative QY of 61% versus the parent nanocrystals in octane. In general, the absolute QY of the aqueous PIL-coated CdSe/CdS nanocrystals prepared fell between 50% and 70%. Addition of the ZnS shell did not confer an added benefit. Importantly, the PIL-coated samples were quite robust and were be stored under ambient lighting and temperature conditions for an extended period (months) with little change in properties. In addition to the organic surface coatings described above, silica-coated single CdSe/CdS nanocrystals were prepared via an inverse-micelle method (total hydrodynamic diameter was controlled in the range of 20-70 nm). These displayed ~40% QY in aqueous solution. See, for example, Popović, Z., et al., *Angew. Chem. Int. Ed.* **2010**, *49*, 8649-8652, which is incorporated by reference in its entirety.

Example 5: Time-resolved PL measurements. PL decay measurements for the nanocrystals were made using the frequency doubled (400 nm) output of a sub-picosecond chirped-pulse amplified Ti:sapphire laser system that was previously described (see Loh, Z.-H. et al. *J. Phys. Chem. A* 2002, 106, 11700-11708, which is incorporated by reference in its entirety). The detector was a Hamamatsu C4334 Streak Scope streak camera. Samples were illuminated in 2 mm pathlength cuvettes at a repetition rate of 1 kHz with vigorous stirring, and the observed changes in decay kinetics with power were reversible.

For single nanocrystal blinking experiments, CdSe(CdS) nanocrystals were spun from a dilute toluene/polymethylmethacrylate solution onto a cover glass (Electron Microscopy Sciences). Individual nanocrystals were observed by confocal epifluorescence microscopy through a 100x, 1.40 NA oil immersion objective (Nikon). The nanocrystals were excited with a continuous-wave Ar^+ laser at 514 nm and the emission was collected using an avalanche photodiode (Perkin Elmer).

Time-resolved PL spectroscopy was employed to characterize the excited state decay process in CdSe/CdS core/shell samples displaying high ensemble QY. FIGS. 5A-5B displays the ensemble PL decay in hexanes at room temperature, excited at low power (exciton density $n < 0.1$) with pulsed 400 nm radiation from a Ti:sapphire laser and recorded using a streak camera. The decay trace was well-described with a single

exponential lifetime τ of ~26 ns. Fluorescence intermittency (blinking) measurements have previously shown that in single nanocrystals, intensity fluctuations are chiefly due to time-varying nonradiative rates and that at maximally bright timepoints, nanocrystals can display near-unity QY and monoexponential PL decays dominated by the radiative recombination rate. See, e.g., Schlegel, G. et al., *Phys. Rev. Lett.* 2002, 88, 137401; Fisher, B. R., et al., *J. Phys. Chem. B* 2004, 108, 143-148; and Spinicelli, P., et al., Phys. Rev. Lett. 2009, 102, 136801; each of which is incorporated by reference in its entirety. An ensemble nanocrystal sample displaying near-unity QY was therefore expected to show largely mono-exponential excited-state decay kinetics because the radiative decay rate, determined by band-edge electronic structure (see Efros, A. L. et al., *Phys. Rev. B* J1 - PRB 1996, 54, 4843 LP - 4856, which is incorporated by reference in its entirety), should be homogeneous in a structurally homogeneous sample. The mono-exponential decay observed at low excitation power was thus consistent with expectations based on the high ensemble QY, but was also indicative of consistent radiative rates among the ensemble population

When the nanocrystals were excited at high fluence (average exciton density per particle $n \approx 2$), an intense decay component was observed with a spectrum similar to that at low fluence and a lifetime of < 100 ps (FIGS. 6A-6D); this was interpreted as a rapid biexciton decay due to Auger recombination. See, for example, Klimov, V. I., et al., *Science* 2000, 290, 314-317; and Fisher, B., et al., *Phys. Rev. Lett.* 2005, 94, 087403; each of which is incorporated by reference in its entirety.

To characterize blinking in our high QY samples, single nanocrystals were observed under continuous-wave excitation at 514 nm. Representative intensity traces (FIGS. 7A, 7C Fig. 6a,c) revealed well-resolved binary blinking between on- and off-state values, and high on-time fractions of 93% (FIG. 7A) and 90% (FIG. 7C). All nanocrystals observed in each sample displayed on-time fractions > 60% with the majority > 80% (FIGS. 7B, 7D).

Suppression of blinking in CdSe/CdS core/shell nanocrystals is manifested by (1) large on-time fractions and (2) "gray" off states that display appreciable QY. See, e.g., Chen, Y. et al., *J. Am. Chem. Soc.* **2008**, *130*, 5026-5027; Mahler, B., et al., *Nat Mater* **2008**, *7*, 659-664; and Spinicelli, P., et al., *Phys. Rev. Lett.* **2009**, *102*, 136801; each of which is incorporated by reference in its entirety. Despite single-particle fluorescence data indicating high on-time fractions and a near-unity QY with mono-exponential decay

in the on state, the reported ensemble QYs are 50-70%, (see Chen; and Spinicelli) indicating that the high fluence single-particle QY may not be representative of ensemble behavior at lower fluence. Models for fluorescence intermittency in nanocrystals have often proposed that the off state is characterized by the persistent presence of extra carrier(s) in one of the band-edge spherical-well states (resulting in an off-state QY that is limited by Auger recombination), or by the opening of a non-radiative decay pathway via localized trap state(s). See, for example, Efros, A.L., et al., *Phys. Rev. Lett.* **1997**, *78*, 1110; and Frantsuzov, P.A., et al., *Phys. Rev. Lett.* **2009**, *103*, 207402, each of which is incorporated by reference in its entirety. Recent work indicates that in nanocrystal systems with weaker and/or gentler core/shell potential profiles, including CdSe/CdS with thick shells, the Auger rate for multiexciton states can be suppressed (Garcia-Santamaria, F., et al., *Nano Letters* **2009**, *9*, 3482-3488, which is incorporated by reference in its entirety).The increase in off-state QY in thick-shelled CdSe/CdS nanocrystals may be a unique feature associated with a suppressed Auger rate due the band-edge electronic structure in such nanocrystals; if so it would indicate that Auger recombination is the dominant quenching mechanism in such nanocrystals in the off state (which does *not* appear to be the case for QDs with ZnS shells at low fluence--see Zhao, J., et al., *Phys. Rev. Lett.* **2010**, *104*, 157403; and Rosen, S., et al., *Phys. Rev. Lett.* **2010**, *104*, 157404, each of which is incorporated by reference in its entirety). The large blinking modulation depth (> 90%) and short biexciton lifetime in our samples stand in contrast to the "gray" off-states and longer biexciton lifetimes obtained for thicker shells; the short biexciton lifetime may also be a function of the relatively small (< 2 nm) core radius used in our samples.

The on-time fraction is determined by the mechanism of switching between on and off states, which invokes interaction with localized states in both models. Thick shells can be effective in spatially isolating the core from the surface, as reflected in ensemble measurements that show reduced sensitivity of QY to surface ligand-exchange reactions in CdSe/CdS nanocrystals for 19 monolayer shell thickness, (Chen, Y., et al., *J. Am. Chem. Soc.* **2008**, *130*, 5026-5027, which is incorporated by reference in its entirety) and this has been invoked in explaining the high on-time fractions noted among subpopulations in thick-shell CdSe/CdS QD samples. Here it was found that, given adequate surface passivation, a high on-time fraction was achieved in nanocrystals with thinner shells that do not isolate the core.

WHAT IS CLAIMED IS:

1. A semiconductor nanocrystal having a photoluminescent quantum yield of at least 90%.

2. The semiconductor nanocrystal of claim 1, wherein the semiconductor nanocrystal comprises a core including a first semiconductor material and a shell including a second semiconductor material.

3. The semiconductor nanocrystal of claim 2, wherein the first semiconductor material is ZnS, ZnSe, ZnTe, CdS, CdSe, CdTe, HgS, HgSe, HgTe, AlN, AlP, AlAs, AlSb, GaN, GaP, GaAs, GaSb, GaSe, InN, InP, InAs, InSb, TlN, TlP, TlAs, TlSb, PbS, PbSe, PbTe, or a mixture thereof.

4. The semiconductor nanocrystal of any one of claims 2-3, wherein the second semiconductor material is ZnS, ZnSe, ZnTe, CdS, CdSe, CdTe, HgS, HgSe, HgTe, AlN, AlP, AlAs, AlSb, GaN, GaP, GaAs, GaSb, GaSe, InN, InP, InAs, InSb, TlN, TlP, TlAs, TlSb, PbS, PbSe, PbTe, or a mixture thereof.

5. The semiconductor nanocrystal of any one of claims 1-4, wherein the semiconductor nanocrystal is a member of a population of semiconductor nanocrystals, wherein the population exhibits photoluminescence with a full width at half max (FWHM) of less than 30 nm.

6. The semiconductor nanocrystal of any one of claims 2-5, wherein the first semiconductor material is CdSe.

7. The semiconductor nanocrystal of claim 6, wherein the second semiconductor material is CdS.

8. A method of making a semiconductor nanocrystal comprising:

forming a nanocrystal core including a first semiconductor material; and

sequentially contacting the nanocrystal core with an M-containing compound and an X donor, thereby forming a second semiconductor material on a surface of the nanocrystal core;

wherein at least one of the M-containing compound and the X donor is substoichiometric with respect to forming a monolayer on the nanocrystal core.

9. The method of claim 8, further comprising repeating the step of sequentially contacting the nanocrystal core with an M-containing compound and an X donor.

10. The method of any one of claims 8-9, wherein both the M-containing compound and the X donor are substoichiometric with respect to forming a monolayer on the nanocrystal core.

11. The method of any one of claims 8-10, wherein the M-containing compound is selected to react quantitatively.

12. The method of any one of claims 8-11, wherein the X donor is selected to react quantitatively.

13. The method of any one of claims 8-12, wherein the first semiconductor material is ZnS, ZnSe, ZnTe, CdS, CdSe, CdTe, HgS, HgSe, HgTe, AlN, AlP, AlAs, AlSb, GaN, GaP, GaAs, GaSb, GaSe, InN, InP, InAs, InSb, TlN, TlP, TlAs, TlSb, PbS, PbSe, PbTe, or a mixture thereof.

14. The method of any one of claims 8-13, wherein the second semiconductor material is ZnS, ZnSe, ZnTe, CdS, CdSe, CdTe, HgS, HgSe, HgTe, AlN, AlP, AlAs, AlSb, GaN, GaP, GaAs, GaSb, GaSe, InN, InP, InAs, InSb, TlN, TlP, TlAs, TlSb, PbS, PbSe, PbTe, or a mixture thereof.

15. The method of any one of claims 8-14, wherein the first semiconductor material is CdSe.

16. The method of claim 15, wherein the second semiconductor material is CdS.

17. The method of any one of claims 8-16, wherein the X donor is bis(trimethylsilyl)sulfide.

18. A population of semiconductor nanocrystals, wherein the population exhibits photoluminescence with a quantum yield of at least 90% and a full width at half max (FWHM) of less than 30 nm.

19. The population of claim 18, wherein the wherein the population exhibits photoluminescence with a quantum yield of at least 95%.

20. The population of claim 18, wherein the wherein the population exhibits photoluminescence with a quantum yield of at least 98%.

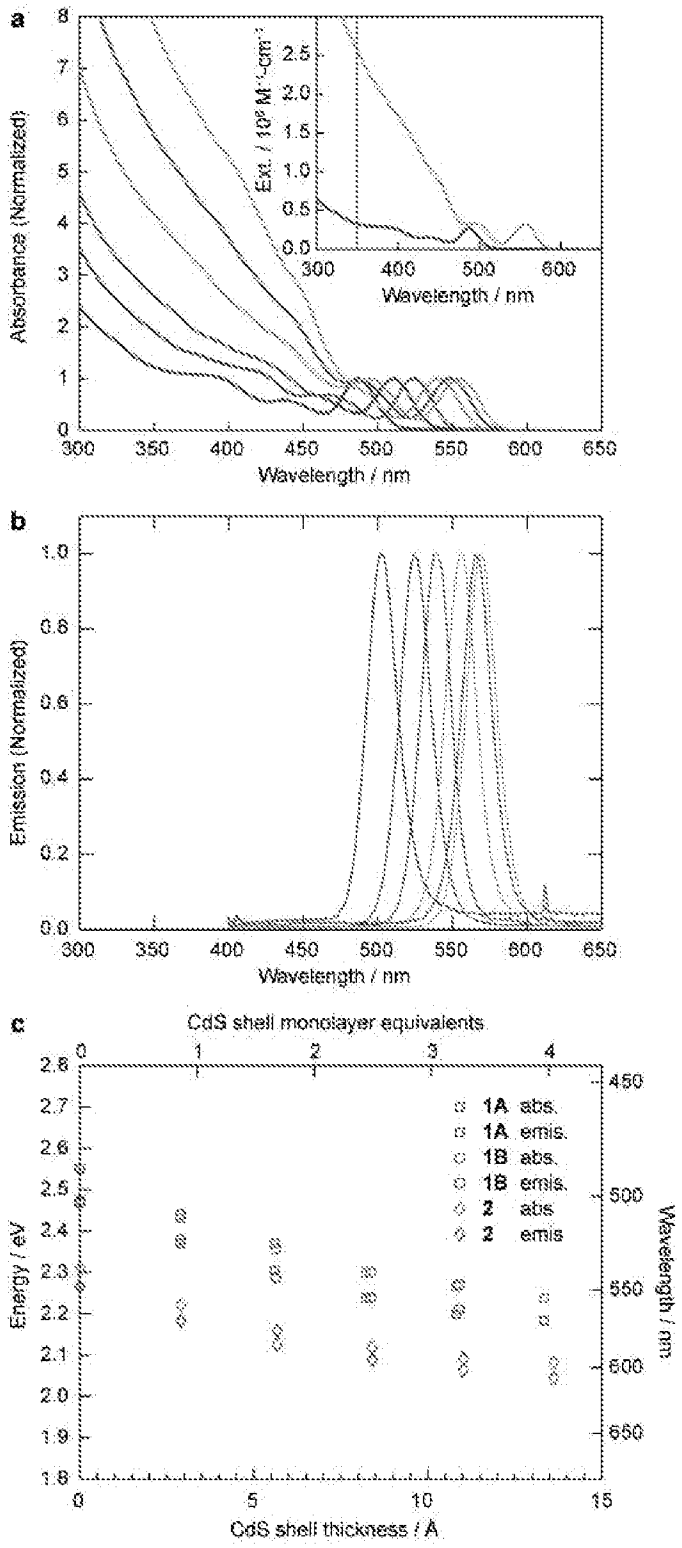
a
Absorbance (Normalized)
Wavelength / nm
Ext. / 10⁵ M⁻¹·cm⁻¹
Wavelength / nm
b
Emission (Normalized)
Wavelength / nm
c
CdS shell monolayer equivalents
Energy / eV
Wavelength / nm
CdS shell thickness / Å
1A abs.
1A emis.
1B abs.
1B emis.
2 abs.
2 emis

FIG. 1

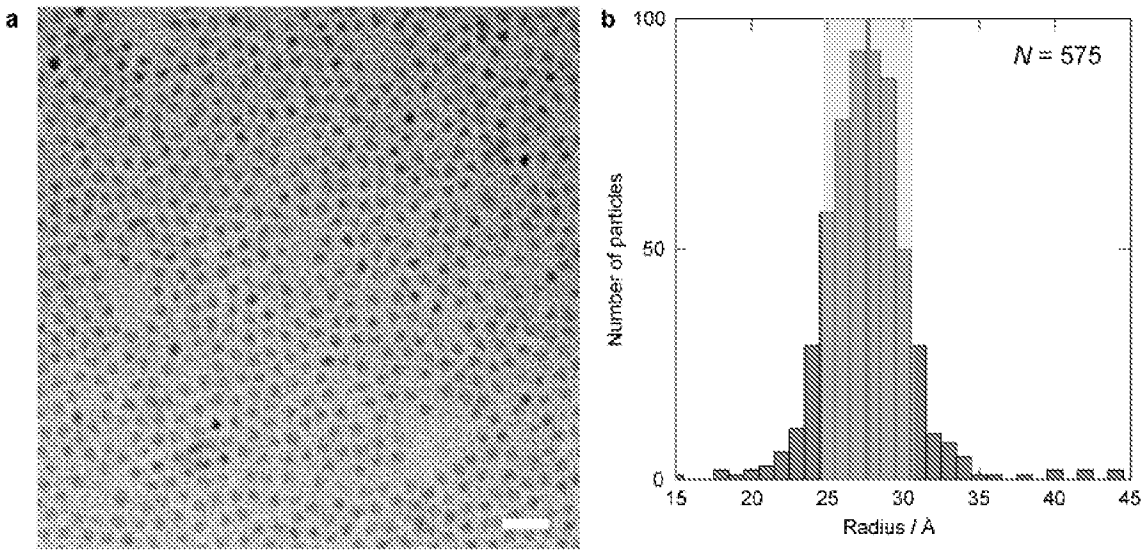
a
b
N = 575
Number of particles
Radius / Å
0
50
100
15
20
25
30
35
40
45

FIG. 2

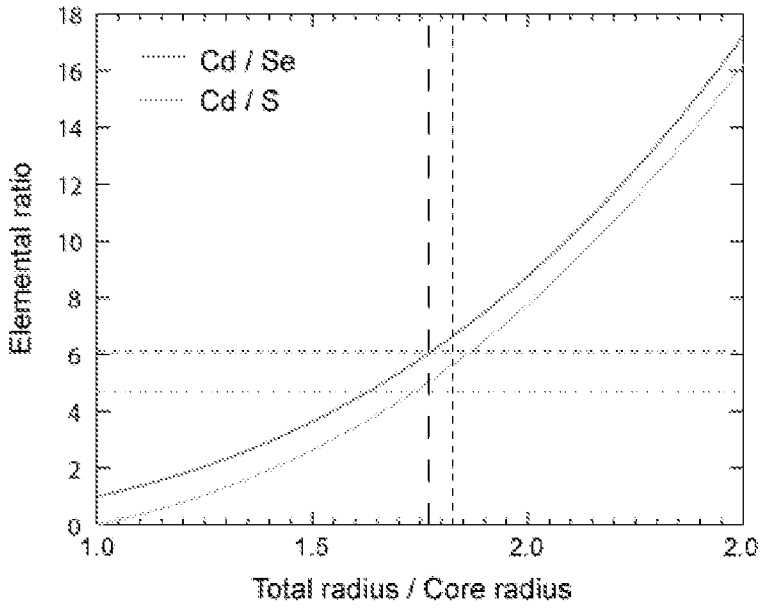
Cd / Se
Cd / S
Elemental ratio
Total radius / Core radius
0
2
4
6
8
10
12
14
16
18
1.0
1.5
2.0
2.0

FIG. 3

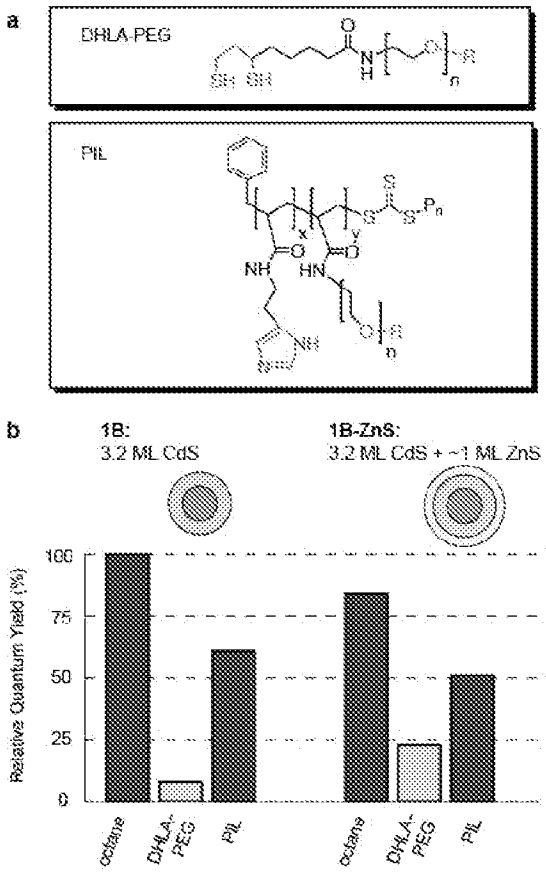
a
DHLA-PEG
PIL
b
1B:
3.2 ML CdS
1B-ZnS:
3.2 ML CdS + ~1 ML ZnS
Relative Quantum Yield (%)
100
75
50
25
0
octane
DHLA-PEG
PIL
octane
DHLA-PEG
PIL

FIG. 4

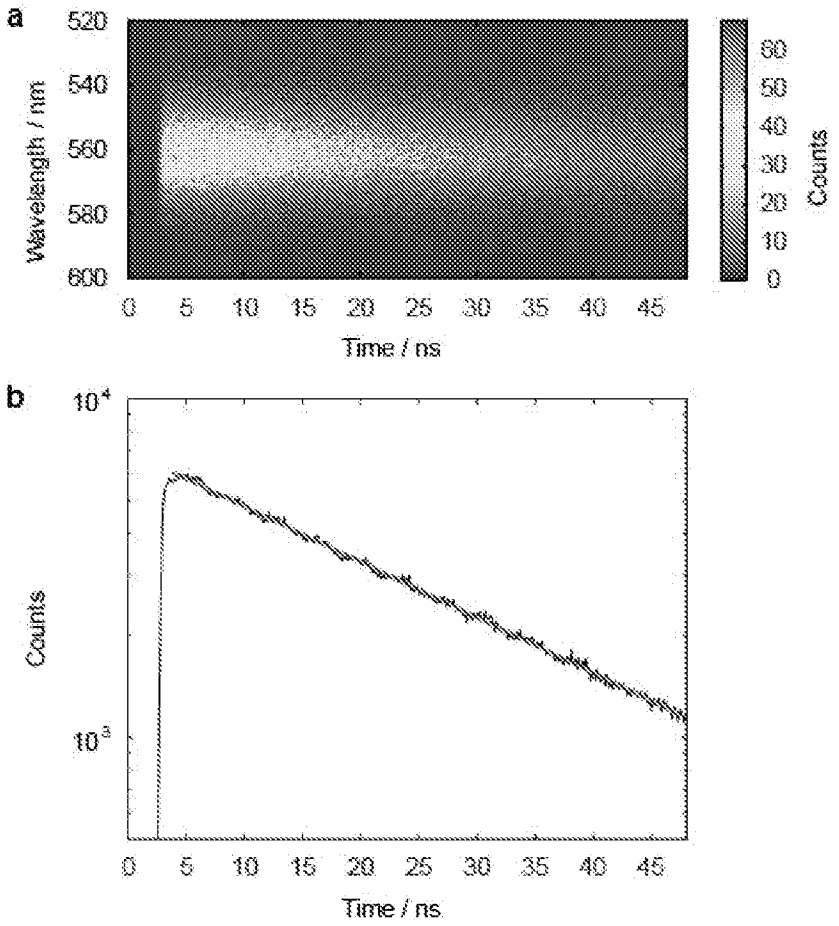
a
520
540
560
580
600
Wavelength / nm
0 5 10 15 20 25 30 35 40 45
Time / ns
60
50
40
30
20
10
0
Counts
b
10^4
10^3
Counts
0 5 10 15 20 25 30 35 40 45
Time / ns

FIG. 5

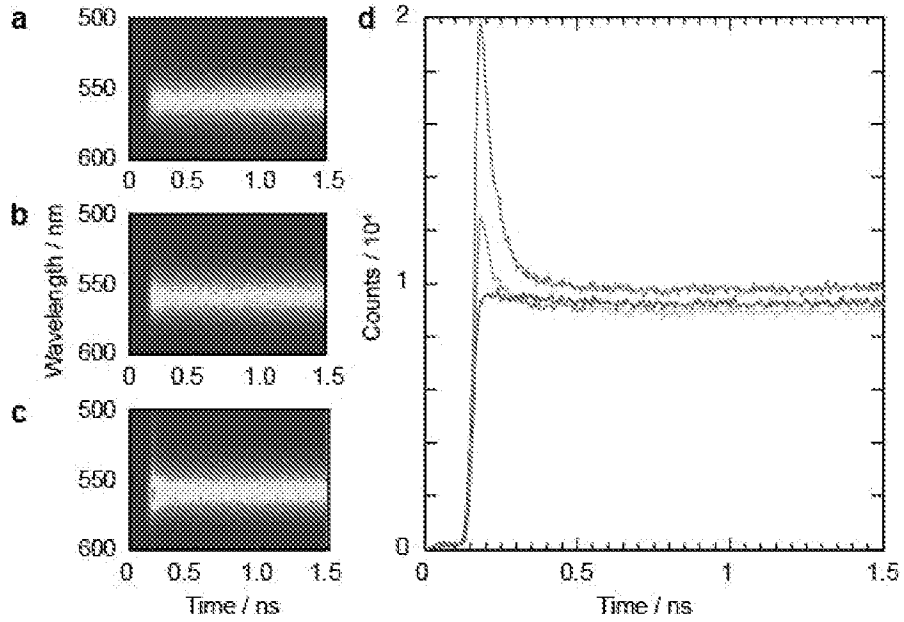
a
b
c
d
Wavelength / nm
Time / ns
Counts / 10⁴
Time / ns

FIG. 6

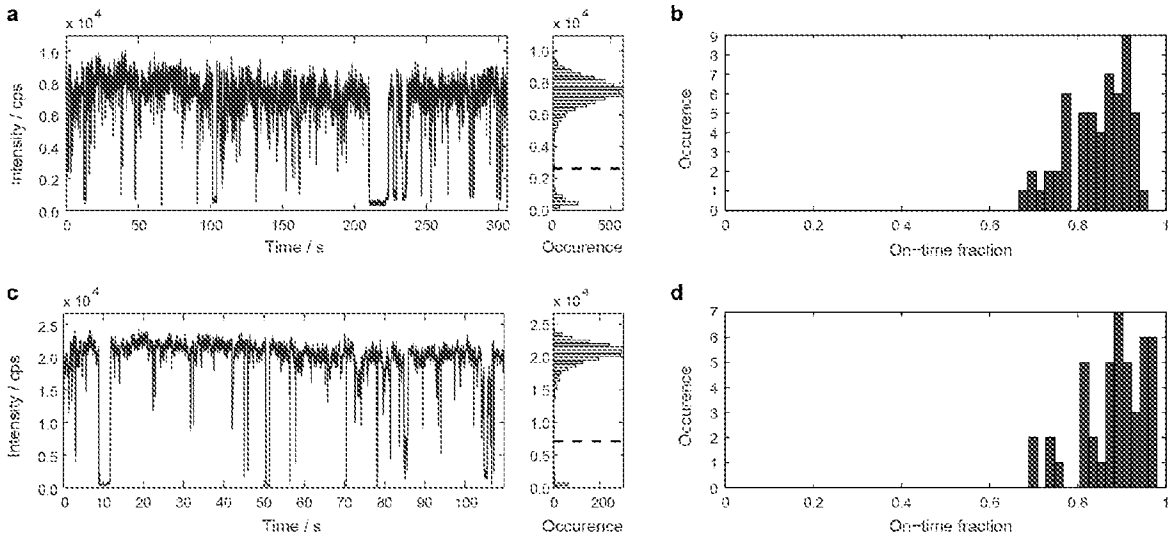
a
b
c
d
Intensity / cps
Time / s
Occurence
On-time fraction

FIG. 7

INTERNATIONAL SEARCH REPORT

International application No
PCT/US2011/048299

A. CLASSIFICATION OF SUBJECT MATTER
INV. C09K11/58 C09K11/88
ADD.

According to International Patent Classification (IPC) or to both national classification and IPC

B. FIELDS SEARCHED

Minimum documentation searched (classification system followed by classification symbols)
C09K G01N

Documentation searched other than minimum documentation to the extent that such documents are included in the fields searched

Electronic data base consulted during the international search (name of data base and, where practical, search terms used)
EPO-Internal, INSPEC, COMPENDEX, WPI Data

C. DOCUMENTS CONSIDERED TO BE RELEVANT

Category*	Citation of document, with indication, where appropriate, of the relevant passages	Relevant to claim No.
X	JAMES MCBRIDE ET AL: "Structural Basis for Near Unity Quantum Yield Core/Shell Nanostructures", NANO LETTERS, vol. 6, no. 7, 9 June 2006 (2006-06-09), pages 1496-1501, XP55013818, ISSN: 1530-6984, DOI: 10.1021/nl060993k cited in the application the whole document ----- -/--	1-20

[X] Further documents are listed in the continuation of Box C.

[X] See patent family annex.

* Special categories of cited documents :

"A" document defining the general state of the art which is not considered to be of particular relevance

"E" earlier document but published on or after the international filing date

"L" document which may throw doubts on priority claim(s) or which is cited to establish the publication date of another citation or other special reason (as specified)

"O" document referring to an oral disclosure, use, exhibition or other means

"P" document published prior to the international filing date but later than the priority date claimed

"T" later document published after the international filing date or priority date and not in conflict with the application but cited to understand the principle or theory underlying the invention

"X" document of particular relevance; the claimed invention cannot be considered novel or cannot be considered to involve an inventive step when the document is taken alone

"Y" document of particular relevance; the claimed invention cannot be considered to involve an inventive step when the document is combined with one or more other such documents, such combination being obvious to a person skilled in the art.

"&" document member of the same patent family

Date of the actual completion of the international search	Date of mailing of the international search report
5 December 2011	13/12/2011

Name and mailing address of the ISA/	Authorized officer
European Patent Office, P.B. 5818 Patentlaan 2 NL - 2280 HV Rijswijk Tel. (+31-70) 340-2040, Fax: (+31-70) 340-3016	Mehdaoui, Imed

INTERNATIONAL SEARCH REPORT

International application No
PCT/US2011/048299

C(Continuation). DOCUMENTS CONSIDERED TO BE RELEVANT

Category*	Citation of document, with indication, where appropriate, of the relevant passages	Relevant to claim No.
X	PENG X ET AL: "Epitaxial growth of highly luminescent CdSe/CdS core/shell nanocrystals with photostability and electronic accessibility", JOURNAL OF THE AMERICAN CHEMICAL SOCIETY, AMERICAN CHEMICAL SOCIETY, WASHINGTON, DC; US, vol. 119, 1 January 1997 (1997-01-01), pages 7019-7029, XP002261067, ISSN: 0002-7863, DOI: 10.1021/JA970754M cited in the application the whole document	1-20
X	JIAN WANG ET AL: "Preparation of Highly Luminescent CdTe/CdS Core/Shell Quantum Dots", CHEMPHYSCHEM, vol. 10, no. 4, 9 March 2009 (2009-03-09), pages 680-685, XP55013848, ISSN: 1439-4235, DOI: 10.1002/cphc.200800672 the whole document	1-20
X	US 2010/044636 A1 (RAMPRASAD DORAI [US] ET AL) 25 February 2010 (2010-02-25) claims 1-43; example 1B	1-20

INTERNATIONAL SEARCH REPORT

Information on patent family members

International application No
PCT/US2011/048299

Patent document cited in search report	Publication date	Patent family member(s)	Publication date
US 2010044636 A1	25-02-2010	US 2010044636 A1	25-02-2010
		WO 2008063658 A2	29-05-2008